Modelling hydro-mechanical reinforcements of plants to slope stability

Ni, J J ; Leung, A. K.; Ng, C. W. W.; Shao, W

Published in:
Computers and Geotechnics

DOI:
10.1016/j.compgeo.2017.09.001

Publication date:
2018

Document Version
Publisher's PDF, also known as Version of record

Computers and Geotechnics 95 (2018) 99–109

Contents lists available at ScienceDirect

Computers and Geotechnics

journal homepage: www.elsevier.com/locate/compgeo

Research Paper

Modelling hydro-mechanical reinforcements of plants to slope stability

J.J. Ni [a], A.K. Leung [b,*], C.W.W. Ng [a], W. Shao [c]

[a] Department of Civil and Environmental Engineering, The Hong Kong University of Science and Technology, Hong Kong Special Administrative Region
[b] Division of Civil Engineering, School of Science and Engineering, University of Dundee, Dundee, Scotland, UK
[c] College of Hydrometeorology, Nanjing University of Information Science and Technology, Nanjing, Jiangsu, China

ARTICLE INFO

Article history:
Received 5 March 2017
Received in revised form 18 June 2017
Accepted 5 September 2017
Available online 14 October 2017

Keywords:
Plant transpiration
Matric suction
Slope stability
Mechanical reinforcement

ABSTRACT

The study investigates plant reinforcement to the stability of coarse-grained soil slopes, exploring the relative contribution of mechanical root reinforcement and hydrological effects of plant-induced matric suction. A numerical model is used to capture both mechanical root reinforcement and hydrological effects, including evapotranspiration with different root architectures and root-induced changes in soil water retention curve and hydraulic conductivity. Mechanical reinforcement is effective only in shallow depths, where the most root biomass exists. Hydrological reinforcement is much more significant in deeper depths (>1 m), but this effect could vanish due to root-induced increase in hydraulic conductivity.

1. Introduction

Soil bioengineering using vegetation has been recognised as an environmentally friendly engineering method for slope stabilisation. A well-known effect of roots on slope stability is the mechanical reinforcements by roots in shallow soil. Plant roots which could sustain tension permeate into soil pore space and increase shear strength of the soil-root composite. In past decades, the mechanical root reinforcement has been extensively quantified experimentally and analytically [1–4] and this effect is usually included in slope stability calculation [5–9]. The contribution of mechanical reinforcement to soil strength depends not only on the root biomechanical properties but also on the amount of roots available in rooted zone. Field studies [10,11] reported that for natural plants, root biomass is mainly concentrated in the top 0.5 m, below which the root number reduces substantially depending on root architecture. Mechanical reinforcement is thus considered to be especially effective for resisting surface erosion and shallow slope stabilisation.

Hydrological reinforcement via evapotranspiration (*ET*) has also been shown to be important to slope stability [10,12–17]. ET is defined as the combined loss of water from a given area, and during a specified period of time, by evaporation from the soil surface and by transpiration from plants [18]. Various field and laboratory studies reported that the antecedent drying effects by ET before rainfall could induce a significant amount of matric suction and hence preserve suction in the soil (between 5 and 150 kPa; depending on the types of soil and plant) after rainfalls [14,19–23]. Centrifuge model tests conducted by Ng et al. [15] have shown that neglecting the effects of ET before rainfall could result in an underestimation of factor of safety (*FS*) by up to 50% after rainfalls. Suction induced/preserved did not only reduce soil hydraulic conductivity (hence infiltration; [24]) but also increase soil shear strength [25]. When subject to prolonged rainfall, although matric suction is likely to have been dropped to zero in shallow depths, it is not uncommon to see some creditable amount of suction preserved in deeper depths (i.e., 1–2 m; [14,19,26]), where sliding mode of slope failure typically happens. In fact, *ET* did not remove soil moisture only within the root zone, but also could extend its influence zone of suction to a much deeper depth below the root zone for up to four times of the root depth [13,22,23,27].

Hydrological effects of vegetation should not collectively refer to only the antecedent effects due to *ET*-induced matric suction. Previous studies have revealed that the presence of plant roots in the soil could cause a change in soil hydraulic properties [20,28–31]. Experimental work reported by Scanlan and Hinz [32], Scholl et al. [29] and Leung et al. [20] have all shown that the presence of roots affects the water retention capacity, hence the shape of soil water retention curve (SWRC), especially in low suction ranges. Ng et al. [31] develops a model to explain the root effects as the change in void ratio of coarse-grained soils due to physical root occupancy in soil pore space. The effects of vegetation on another soil hydraulic property, infiltration rate and hydraulic conductivity, on the other hand, also received some attention in the literature [19,26,28,30,33]. In general, the findings are inconclusive because

* Corresponding author.
E-mail address: a.leung@dundee.ac.uk (A.K. Leung).

https://doi.org/10.1016/j.compgeo.2017.09.001
0266-352X/

Nomenclature

A_r	sum of total root cross-section area
A_s	soil cross-section area
A	fitting parameter for the relationship between k_s and e
B	fitting parameter for the relationship between k_s and e
c'	effective cohesion
c_r	root cohesion
e	void ratio
e_0	void ratio of parent soil
FS	factor of safety
$G(\eta)$	parameter related to root distribution
h	water pressure head
H	depth of the water table
k_s	saturated hydraulic conductivity
$k(h)$	permeability function (as a function of water pressure head)
$k(\psi)$	permeability function (as a function of soil matric suction)
m_1	parameter controlling the shaper of SWRC
m_2	parameter controlling the shaper of SWRC
m_3	parameter related to the AEV of soil
m_4	parameter related to the AEV of soil
V_r	total volume of roots
V_s	unit volume of soil
RAI	root area index
RAR	root area ratio
R_v	root volume ratio
S	degree of saturation
S_r	residual degree of saturation
S_T	sink term
S_{max}	maximum sink when transpiration is not suppressed by oxygen and water stresses
t	time
T_r	average root tensile strength
u_a	pore-air pressure
u_w	pore-water pressure
z	soil depth
Z	pre-defined depth of a slip surface
ψ	soil matric suction
ξ	angle of shear distortion of roots
$\alpha(\psi)$	transpiration reduction function
$\eta(z)$	root distribution along depth
β	inclination of the infinite slope
γ_s	dry unit weight of vegetated soil
γ_w	unit weight of water
k	parameter that represents the radiation interception by plant leaves
θ	volumetric water content
σ	total normal stress
τ_b	shear strength of bare soil
ϕ'	effective friction angle

some studies showed a decrease in saturated hydraulic conductivity (k_s), while some showed an increase. Certainly, these hydrological effects of plant (herein defined as root-induced changes in soil hydraulic properties) could play a role in soil hydrology and stability, but they have generally been ignored in most of the existing stability analysis.

Because of the lack of research, hydrological reinforcements of vegetation (i.e., a combination of the effects of *ET* and root-induced change in soil hydraulic properties) are often neglected when quantifying the stability of a vegetated slope. Liu et al. [34] is one of the rare studies, which attempt to estimate the effect of *ET*-induced suction on slope stability. Other hydrological effects and mechanical root reinforcement are not considered. In fact, the field study carried out by Pollen-Bankhead and Simon [12] showed that while mechanical reinforcement increased the *FS* of a streambank by 25%, the effects of *ET* -induced suction translated in a much more significant increase in *FS* by 52%. Rahardjo et al. [14] also reported that while the control fallow slope had 25.9% drop in *FS* after 24 h of rainfall, the vegetated slopes had a decrease of only less than 7% in *FS*. More research is thus needed to clarify the relative importance between the mechanical and hydrological reinforcements of plant roots to slope stability.

The aim of this paper is to develop a model that can quantify the mechanical and hydrological effects and their relative contribution on the stability of an unsaturated vegetated coarse-grained soil slope. In this model, the hydrological effects of vegetation considered include (i) *ET*; (ii) root-induced change in soil water retention curve (SWRC) and (iii) root-induced change in saturated hydraulic conductivity (k_s). The model is validated by two sets of field double-ring infiltration tests on both bare and vegetated grounds. Using the validated model, a series of parametric studies on the effects of different root architectures on soil hydraulic properties, soil hydrology (in terms of matric suction) and slope stability (in terms of *FS*) are conducted. The relative significance of the mechanical and hydrological contributions of roots to the slope stability is then investigated and highlighted.

2. Materials and methods

In order to assess the stability of an unsaturated vegetated slope, soil hydrology and its change due to the hydrological effects of vegetation needs to be considered. Therefore, two stages of calculation are conducted. The first stage is to determine the pore-water pressure distribution through transient seepage analysis. The calculated results are then used in the second stage for slope stability analysis using the limit equilibrium method.

2.1. Hydrological model for an unsaturated vegetated soil

Consider one-dimensional (1D) transient seepage in an unsaturated soil along the depth, z, Richard's equation is used to describe the process

$$\frac{d\theta}{dt} = \frac{d}{dz}\left[k(h)\left(\frac{dh}{dz}+1\right)\right] - S_T(\psi \text{ or } h, z) \tag{1}$$

where θ is the volumetric water content; t is the elapsed time, h is the water pressure head; $k(h)$ is the soil hydraulic conductivity function as a function of h or matric suction ($\psi = -h\gamma_w$, where γ_w is the unit weight of water); and S_T is the sink term, which represents the volume of water transpired by a plant integrating over the entire root zone for a given time interval [35]. Mathematically, S_T may be expressed as follows:

$$S_T(\psi \text{ or } h, z) = \alpha(\psi)\cdot S_{max} = \alpha(\psi)\cdot G(\eta)\cdot PT \tag{2}$$

where $\alpha(\psi)$ is known as transpiration reduction function, ranging from 0 to 1; $G(\eta)$ is related to root architecture, $\eta(z)$; and S_{max} is the maximum sink when transpiration is not suppressed by oxygen and water stresses (i.e., $\alpha(\psi) = 1$; [35]. Under this condition, the plant undergoes potential transpiration (PT; maximum amount of water that plants could extract water from the soil [36]). Otherwise, the amount of plant-water uptake (S_T) would depend on both the magnitude and distribution of suction within the root zone.

In order to solve Eq. (1), two hydraulic properties are required to assess transient seepage in unsaturated soil; $k(h)$ and soil water retention curve (SWRC; which depicts the relationship between ψ and degree of saturation, S). In addition to the hydrological effects of root-water uptake as captured by Eq. (2), Ng et al. [31] suggests that the presence of fine roots (i.e., diameter less than 2 mm; [37] could modify the SWRC of coarse-grained soil due to the change in soil void ratio. Based on the existing field and laboratory data, they assume that part of the soil pore space is occupied by certain volume of roots. By considering a phase diagram of an unsaturated rooted soil, Ng et al. [31] proposed the following equation to model the root-induced change in void ratio, e

$$e = \frac{e_0 - R_v(1+e_0)}{1 + R_v(1+e_0)} \tag{3}$$

where e_0 is the void ratio before root permeation (i.e., bare soil); R_v is the root volume ratio, which is defined as the total volume of roots (V_r) per unit volume of soil (V_s). Eq. (3) is then fed into the void ratio-dependency SWRC equation proposed by Gallipoli et al. [38]:

$$S = \left[1 + \left(\frac{\psi e^{m_4}}{m_3}\right)^{m_2}\right]^{-m_1} \tag{4}$$

where m_1, m_2, m_3 and m_4 are the model parameters. m_1 and m_2 control the shape of SWRC [39], while m_3 and m_4 are related to the air-entry value (AEV) of the soil. It should be noted that the model proposed by Ng et al. [31], however, may not be applicable to fine-grained soils. Root growth in fine-grained soil has shown to cause substantial changes in soil volume, soil aggregation [40] and formation of macro-structures and cracks, the processes of which are all not taken into account in the model. The predictability of Eqs. (3) and (4) has been evaluated by Ng et al. [31].

For $k(\psi)$, it can be expressed by the equation proposed by van Genuchten [39], as follows:

$$k(\psi) = k_s \cdot S^{0.5}\left[1 - \left(1 - S^{\frac{1}{m_1}}\right)^{m_1}\right]^2 \tag{5}$$

where m_1 is identical to that used to define the SWRC in Eq. (4); k_s is the saturated hydraulic conductivity. Some field and laboratory studies [14,27,41–43] show that k_s of vegetated soil could be reduced by the presence of roots, as compared to fallow soil. This is probably because of root occupancy of soil pore space and hence reduction of soil void ratio and hence hydraulic conductivity. The following empirical form of equation [44] may then be used to describe the relationship between k_s and e:

$$k_s = a \cdot \exp(b \cdot e) \tag{6}$$

where a and b are fitting parameters. Eqs. (1)–(6) were implemented by an author-developed script using Matlab. Richard's equation (Eq. (1)) was solved by a fully-implicit finite difference method [45].

2.2. Stability equation of an infinite vegetated soil slope

According to a shear strength theory of an unsaturated soil [46], the shear strength of a bare soil, τ_b, at failure can be calculated as follows:

$$\tau_b = c' + (\sigma - u_a)\tan\varnothing' + (u_a - u_w)\left[(\tan\varnothing')\left(\frac{S - S_r}{1 - S_r}\right)\right] \tag{7}$$

where c' is the effective cohesion; σ is the total normal stress; u_a and u_w are the pore-air and pore-water pressure, respectively (note: $(u_a - u_w)$ is equal to matric suction, ψ); ϕ' is the effective friction angle; S is the degree of saturation, which follows Eq. (4); and S_r is the residual S. The shear strength of an unsaturated soil varies with suction and SWRC. Experimental evident reported by Hossain and Yin [47] showed that the shear strength equation proposed by Vanapalli et al. [46] (Eq. (7)) fitted well with the shearing behaviour of compacted completely decomposed granite (i.e., the same soil type investigated in the present study) for the matric suction range from 0 to 300 kPa. It should be noted that for other soil types, different shear strength equations [48] might be used to more correctly determine the effects of suction on shear strength and factor of safety. For vegetated soil, additional shear strength contributed by the mechanical root reinforcement is commonly considered through the so-called root cohesion, c_r. Wu et al. [1] proposed a semi-empirical expression for c_r, which was later modified by Preti and Schwarz [49]:

$$c_r = 0.4 \cdot (\sin\xi + \cos\xi\tan\varnothing') \cdot T_r \cdot RAR \tag{8}$$

where ξ is the angle of shear distortion in the shear zone at root breakage; T_r is the average root tensile strength; and RAR is the root area ratio, which is defined as the ratio of the sum of total root cross-section area (A_r) to the soil cross-section area (A_s). Wu et al. [1] showed that the term, $(\sin\xi + \cos\xi\tan\varnothing')$, is close to 1.2. Eq. (8) assumes that all the roots break simultaneously, without considering any progressive failure of roots. In order to correct for the overestimation of the root reinforcement due to this assumption, an empirical correction factor of 0.4 is applied by Preti and Schwarz [49]. This factor was calculated by the ratio of average measured root cohesion to predicted values by Wu et al. [1]'s equation. Hence, the shear strength of an unsaturated vegetated soil, τ_r, can be determined by the sum of Eqs. (7) and (8).

Fig. 1 shows the geometry and definition of parameters of an infinite unsaturated vegetated slope with a groundwater table at depth H. Shear stress induced by the self-weight of the vegetated soil at any pre-defined depth of a slip surface, Z, must be balanced by soil shear strength. Based on force equilibrium, FS of an infinite slope with an inclination of β at failure can be expressed as:

$$FS = \frac{c' - u_w\left[(\tan\varnothing')\left(\frac{S-S_r}{1-S_r}\right)\right] + 0.48 \cdot T_r \cdot RAR}{\left[\gamma_s Z + \gamma_w \int_0^Z \theta dz\right]\sin\beta\cos\beta} + \frac{\tan\varnothing'}{\tan\beta} \tag{9}$$

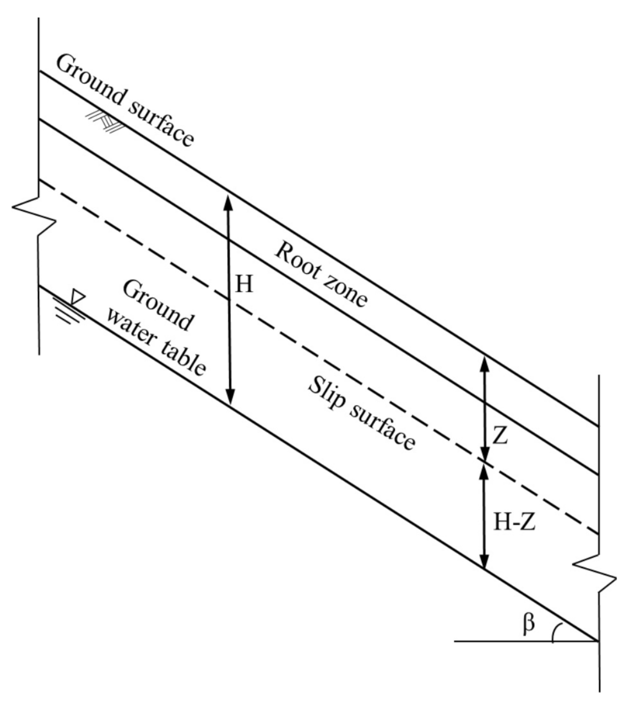

Fig. 1. Definition of the geometry of an infinite vegetated slope.

where γ_s is the dry unit weight of vegetated soil. Hence, by using Eqs. (1)–(9), the coupled effects of (i) mechanical root reinforcement; (ii) hydrological effects of ET and (iii) root-induced change in soil hydraulic properties on the *FS* of an unsaturated vegetated coarse-grained soil slope can be considered simultaneously.

2.3. Calibration and validation of the hydrological model

The hydrological models (i.e., Eqs. (1)–(6)) are validated against two sets of field double-ring infiltration tests conducted by Leung et al. [33] and Ng et al. [31]. These field studies represent two of the rare field datasets that contain sufficient information of both soils and plants for calibrating and validating the hydrological models. Both field studies tested the same coarse-grained soil types (silty sand) and the same plant species (*Schefflera heptaphylla*). In both cases, a constant-head ponding was maintained on the ground surface within the double rings, until a steady-state condition had reached. During testing, ψ from depths of 0.1–0.5 m was monitored by jet-fill tensiometers (Soilmoisture Equipment Corporation; 2725A; ranging from 0 to 80 kPa with accuracy and resolution of 1 kPa). The differences between the two field studies are (i) the initial distribution of matric suction; (ii) the climate conditions during testing (see Table 1); and (iii) the root characteristics.

Before validation, the model parameters involved in the sink term (i.e., Eq. (2)) and the models that capture root-induced change in soil hydraulic properties (i.e., from Eqs. (3)–(6)) are calibrated. In both field experiments, ψ recorded was well below 100 kPa. Feddes et al. [35] suggests that under this condition, plant may transpire without developing much oxygen and water stresses. Hence, it is reasonable to assume $\alpha(\psi)$ to be 1. To calibrate $G(\eta)$, the distributions of R_v of the trees tested in the two studies are needed. As shown in Fig. 2, both R_v profiles are parabola in shape. However, the peak R_v for the trees tested by Ng et al. [31] was higher than that in Leung et al. [33], while the root depth in the former case was 100 mm shorter. In each case, the distribution of $G(\eta)$ is obtained by dividing R_v at each depth by the integration of R_v for the entire root zone up to the root depth.

PT is determined by partitioning the potential evapotranspiration (*PET*) through the Beer-Lambert law [50], as follows:

$$PT = PET(1 - \exp(-k \cdot LAI)) \quad (10)$$

where k is the parameter that represents the radiation interception by plant leaves (taken to be 0.75 for *S. heptaphylla*; [51]); and LAI is the Leaf Area Index, which is 1.8 for the *S. heptaphylla* in both field studies. *LAI* is defined as the ratio of the total leaf area to the projected area of canopy on the soil surface in horizontal plane [52]. The total leaf area was determined by image analysis using an open-source software, ImageJ [53]. Images of each individual tree leaf were taken by a high-resolution camera and were then converted to binary images for obtaining the total leaf area. The projected area of canopy was determined by the circular area, of which the diameter is defined by the maximum lateral spread of tree canopy. Potential evapotranspiration (*PET*) is defined as the maximum amount of *ET* under well (or unlimited) water supply condition [54], which can be calculated by the Penman-Monteith equation [55]. Eq. (10) is commonly used to partition *PT* from *PET* [50,56,57]. It is originally developed for a row grain sorghum (*Sorghum bicolor L.*) canopy in [50]. Recent studies have demonstrated that Eq. (10) is also reasonably applicable to other plant functional groups including trees (*S. heptaphylla*; [20]) and shrubs (*Guapira macrocarpa*; [56]). Using the climate data presented in Table 1, the calculated *PET* for the field tests conducted by Ng et al. [31] and Leung et al. [33] is 0.27 and 0.24 mm/h, respectively. For the given *LAI* of 1.8, the PT calculated by Eq. (10) is found to be 0.20 and 0.18 mm/h for the two cases, respectively. Hence, by subtracting PT from *PET*, the potential evaporation (*PE*, maximum amount of water leaves the soil surface as vapour under well (or unlimited) water supply condition [58]) for the case of Ng et al. [31] and Leung et al. [33] was 0.07 mm/h and 0.06 mm/h, respectively. For the bare soil case, *PE* was estimated by Penman equation [58]. Based on the climate data provided by Ng et al. [31] and Leung et al. [33], the *PE* was 0.12 and 0.11 mm/h, respectively.

In order to calibrate the model parameters in Eq. (4), SWRC of bare soil measured in the field is used. Fig. 3 shows the measured SWRC of the bare silty sand at an e_0 of 0.52. By fitting the data using Eq. (4), the parameters, m_1, m_2, m_3 and m_4 are calibrated to be 0.11, 2.5, 0.30 and 3.64, respectively. By using these calibrated parameters and the known R_v (Fig. 2), SWRC of rooted soil is pre-

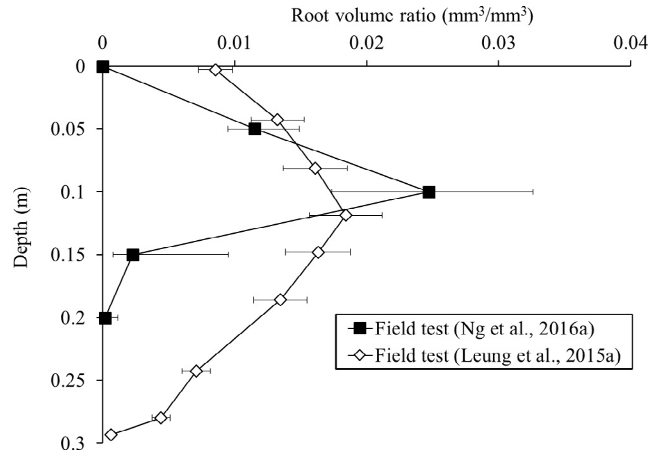

Fig. 2. Variations of measured root volume ratio (R_v) with depth. Error bar represents standard deviation.

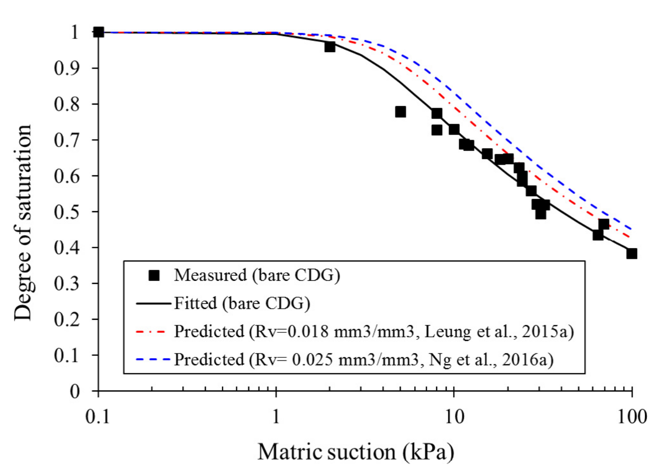

Fig. 3. Soil water retention curves of CDG with and without the presence of roots.

Table 1
Summary of climate data for the field tests conducted by Ng et al. [31] and Leung et al. [33].

Climate data	Ng et al. [31]	Leung et al. [33]
Air temperature (°C)	21.1	17.1
Solar radiation (MJ/m^2/day)	8.8	9.3
Relative humidity (%)	87	81
Wind speed (m/s)	2	2
Potential evapotranspiration (PET; mm/h)*	0.27	0.24
Potential transpiration (PT; mm/h)**	0.20	0.18

* PET calculated by Penman-Monteith equation [55].
** PT calculated by the partitioning equation proposed by Richie (1972; Eq. (10)).

Table 2
Summary of parameters used to define SWRC (Eq. (4)) in the model validation.

Case	Parameters					Root depth [m]	Corresponding R_v [mm^3/mm^3]
	m_1 [–]	m_2 [–]	m_3 [kPa]	m_4 [–]	e_0 [–]		
Leung et al. [20]	0.11	2.5	0.30	3.64	0.52	0.3	0.018
Ng et al. [31]						0.2	0.025

dicted. The predicted SWRCs of root-permeated soil at the depth, where the peak R_v value of 0.018 mm^3/mm^3 (for case [33]; refer to Fig. 2) and 0.025 mm^3/mm^3 (for case [31]) are identified, are shown in Fig. 3. It should be noted that for a known parabolic distribution of R_v, Eqs. (3) and (4) could be used to predict SWRC of rooted soil at different depths within the root zone. Table 2 summarises all the calibrated parameters used to define Eq. (4) in the model validation.

The model parameters for Eq. (6) are calibrated using the data reported by Leung et al. [33], who measured k_s of the silty sand vegetated with *S. heptaphylla* using a double-ring infiltrometer. The relationship between k_s and e (see Fig. 4) is log-linear and is fitted by Eq. (6). The parameters a and b are 6×10^{-10} m/s and 14.8, respectively. Hence, $k(\psi)$ at different depths within the root zone in Eq. (5) can be estimated. For the bare soil at e_0 of 0.52, the k_s is 1.22×10^{-6} m/s.

For the validation of each field study, a 1D soil profile with 4.5 m depth (beyond which bedrock was found in the field) is considered. A constant head of 100 mm is specified as the top boundary for two hours. At the bottom boundary, a constant water table at 4.5 m depth as observed by Leung et al. [33] is set. Based on the field monitoring results, ψ before ponding distributed fairly linearly (shown later). Thus a linear initial distribution of ψ is specified in both cases of simulations.

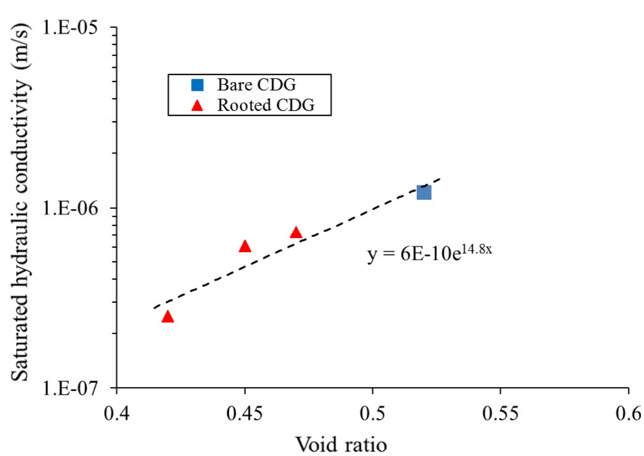

Fig. 4. Relationship between saturated hydraulic conductivity (k_s) and void ratio (e) with and without the presence of roots.

Three simulations are conducted for each field study. The first one is to simulate the ponding test on the bare soil (Case B). In this case, the SWRC and $k(\psi)$ of the bare soil is specified for the entire soil profile. The second and third analyses aim to model the ponding test on the vegetated ground. Thus, a root zone is specified in the top of the soil profile. In the second analysis (Cases V1 and V2 for Leung et al. [33] and Ng et al. [31]), only the effects of ET are modelled, without considering the root-induced changes in SWRC and $k(\psi)$. In other words, the hydraulic properties of the bare soil are specified both within and below the root zone. In the third analysis (Cases VR1 and VR2), both the effects of ET and root-induced changes in the two hydraulic properties are considered. Within the root zone, the modified SWRC and $k(\psi)$ due to the presence of roots are used. Table 3 summarises the input parameters and boundary conditions used in the model validation.

2.4. Parametric study

After validating the hydrological model, parametric study is conducted to study the effects of vegetation on slope stability using Eq. (9). The main objective of the parametric study is to identify the relative importance among the three factors, namely (i) mechanical effects of root reinforcement; (ii) hydrological effects of ET and (iii) root-induced change in soil hydraulic properties, on slope stability. An infinite slope with an angle β of 40° and a thickness (H) of 10 m is considered to be subjected to a rainfall event with a duration of 24 h. The slope geometry chosen for analysis falls within the typical ranges for man-made slopes such as cuttings and embankments in crowded cities like Hong Kong [59] and Singapore [60]. The soil considered in the simulation is completely decomposed granite (CDG; a common soil type typically found in tropical and subtropical regions such as Hong Kong, Brazil and South Korea). The CDG considered in this study has a typical dry unit weight γ_s of 15 kN/m^3, effective cohesion c' of zero and a critical-state friction angle of 37.4° [47,61]. Since the slope angle is higher than the critical-state friction angle, the initial stability of the bare slope (i.e., Case B) is maintained by the hydrostatic matric suction generated by a water table located at 10 m depth. The SWRC and $k(\psi)$ of the CDG are taken to be the same as those adopted in the validation.

Table 3
Summary of input parameters and boundary conditions adopted for model validation.

Simulation ID[a]	Input parameters			Boundary conditions	
	Root depth [m]	PE or PT [mm/h]	SWRC & $k(\psi)$	Top	Bottom
B	N/A	PE: 0.12	Bare soil[b]	Constant water head of 100 mm	Constant groundwater table at 4.5 m depth
V1	0.3	PT: 0.18	Bare soil[b]		
V2	0.2	PT: 0.20			
VR1	0.3	PT: 0.18	Vegetated soil 1[c]		
VR2	0.2	PT: 0.20	Vegetated soil 2[c]		

[a] "B" donates Bare soil, "V" donates Vegetated soil, "R" donates that root-induced changes in soil hydraulic properties is considered in an analysis; "1" and "2" refers to the study by Leung et al. [33] and Ng et al. [31], respectively.
[b] The input soil parameters: m_1 = 0.11, m_2 = 2.5; m_3 = 0.30 kPa, m_4 = 3.64, e_0 = 0.52, k_s = 1.22×10^{-6} m/s.
[c] The SWRC & $k(\psi)$ are calculated by Eqs. (3)–(6) using R_v distributions shown in Fig. 2 and parameters summarized in Table 2.

When vegetation is included, the root depth is considered to be 1 m (typical root depth found in CDG, [11]. The measured T_r of *Schefflera heptaphylla* that was grown in CDG [11] is specified for the entire root zone. The reported values of T_r vary from 3.3 to 85.7 MPa, so a lower and upper bound analysis using the two extreme values are conducted. Four different shapes of R_v distribution within the 1 m-root zone are considered, namely triangular [20], c; Case VE), uniform [36]; Case VU), parabolic [33]; Case VP) and inversely triangular (Case VI) shapes (Fig. 5). For fair comparison, these distributions have the same root depth and the same total root volume. The R_v values in Fig. 5 are derived from the species *S. heptaphylla*, a common species found in Asia [11,62]. Accordingly, the SWRCs of rooted CDG at different depths within the root zone are determined by Eqs. (3) and (4). By assuming that a root is cylindrical in shape, R_v in each case can be converted to *RAR* for calculating the mechanical root reinforcement using Eq. (8). Consider a volume of rooted root at a depth range Δh within the root zone:

$$R_v = \frac{\sum V_r}{V_s} = \frac{\sum (A_r \cdot \Delta h)}{A_s \cdot \Delta h} = \frac{\sum A_r}{A_s} = RAR \qquad (11)$$

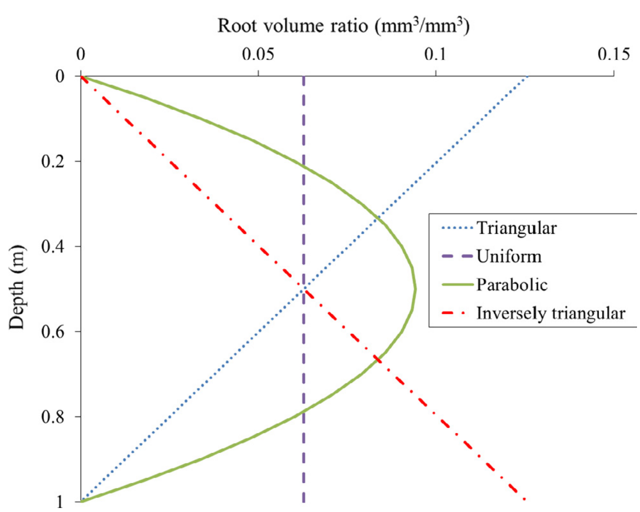

Fig. 5. Four different distributions of root volume ratio (R_v) with depth for parametric study.

It should be noted that for vegetated cases, the root-induced changes in SWRC and $k(\psi)$ take place only in the 1 m-depth root zone, while the soil hydraulic properties below the root zone follow those used for the bare soil case. In all five cases (i.e., Cases B, VT, VU, VP and VI), the same initial distribution of matric suction is considered. A static groundwater table that was parallel to the slope is set at 10 m depth. A hydrostatic distribution of matric suction is hence resulted, having zero value at the base of the slope and a peak value of 100 kPa at the slope surface. It should be noted that ET prior to rainfall is not modelled, as this has been extensively investigated in previous studies [15,16,34,63]. As a result, any differences in pore-water pressure responses between bare and vegetated soil would be solely associated with the effects of ET during rainfall and root-induced changes in soil hydraulic properties within the root zone.

Regarding the hydraulic boundary condition, rainfall infiltration is simulated by applying a constant flux boundary of 394 mm/d at the slope surface for a duration of 24 h (equivalent to the return period of 10 years; [64]. In an attempt to model runoff, at each time step, when the rainfall intensity is higher than the infiltration capacity of the CDG, the flux boundary would be switched to a pressure boundary with a pressure head of 1 mm. Physically, this numerical treatment means that any rainwater that could not infiltrate would discharge in form of surface runoff, leaving a ponding head of a maximum height of 1 mm. On the contrary, when the rainfall intensity is smaller than infiltration capacity, the flux boundary applied would remain unchanged. In order to investigate the significance of *ET* during prolonged rainfall, root-water uptake is considered for the four cases with different R_v profiles through Eq. (2), where (i) $\alpha(\psi)$ is set to be 1.0, (ii) $G(\eta)$ is considered in the same way as the validation and (iii) *PT* is set to be a constant of 0.2 mm/h (as considered in the validation) for the entire raining period of 24 h. For Case B, the *PE* of 0.12 mm/h (as adopted in the validation) is applied to the slope surface during rainfall. Table 4 summarises the analysis plan, input parameters and boundary conditions used in the parametric study.

3. Results and discussion

3.1. Validation results

Fig. 6(a) and (b) show the measured distributions of matric suction obtained from the field tests conducted by Leung et al. [33] and Ng et al. [31], respectively. Before applying the surface

Table 4
Analysis plan, input parameters and boundary conditions adopted in the parametric study.

Simulation ID[a]	Input parameters						Boundary conditions (for hydrological modelling)		
	Hydrological modelling			Stability calculation			Top		Bottom
	Shape of R_v profile in the 1 m root zone	SWRC within root zone	k_s [m/s]	c' [kPa]	ϕ' [°]	c_r [kPa]	PT or PE [mm/h]	Rainfall event	
B	N/A	See Fig.3	1.22×10^{-6}			N/A	PE: 0.12		
VT1			See Figs. 4 and 5						
VT2	Triangular	Follow Eq. (4), R_v distributions in Fig. 5 and parameters in Table 2	$1.3 \times$ Case B	0	37.4	See Eq. (8) and shape of R_v	PT: 0.20	Constant rainfall intensity: 394 mm/d for a duration of 24 h	Constant groundwater table at 10 m depth
VT3			$6.5 \times$ Case B						
VU	Uniform		See Figs. 4 and 5						
VP	Parabolic								
VI	Inverse triangle								

[a] "B" donates Bare soil, "V" donates Vegetated soil, "E", "U", "P" and "I" donates rooted soil with R_v profiles in the shape of exponential, uniform, parabolic and inverse triangle, respectively.

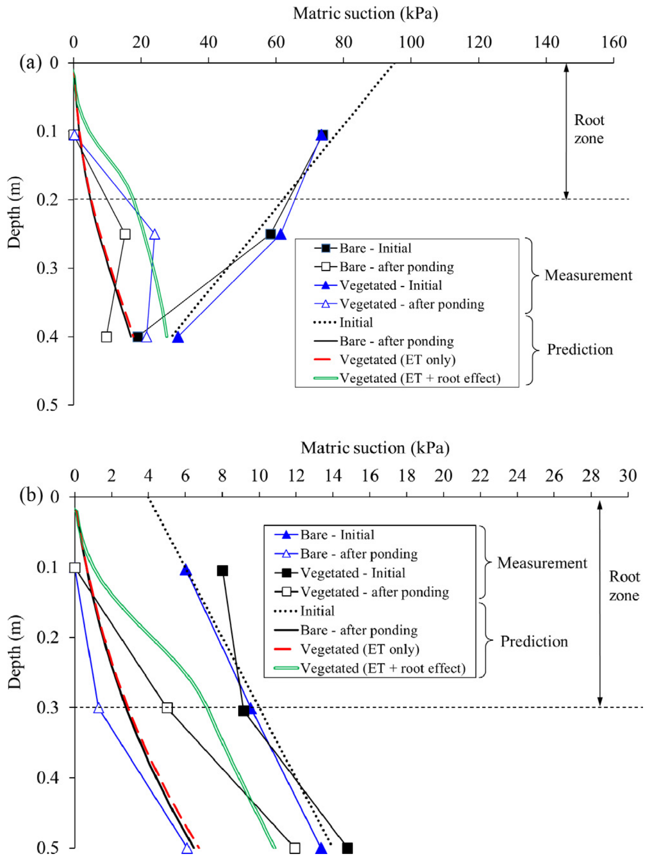

Fig. 6. Comparisons of measured and predicted suction before and after 2-h ponding for the field studies conducted by (a) Ng et al. [31] and (b) Leung et al. [33].

ponding, the initial matric suction between the bare and vegetated grounds is similar to each other, in both tests. After ponding, suction in both the bare and vegetated grounds drops to zero in shallow depths. Although the initial suction between the two field tests is different, the amount of suction preserved below the root zone of the vegetated ground in both cases is always higher than that in the bare ground, by 85–123%.

The simulation results for each field study are superimposed in the respective figure for direct comparison. When the effects of root-induced changes in soil hydraulic properties are ignored and considering only ET, the predicted suction profile of vegetated ground after ponding is almost identical to that of the bare ground,

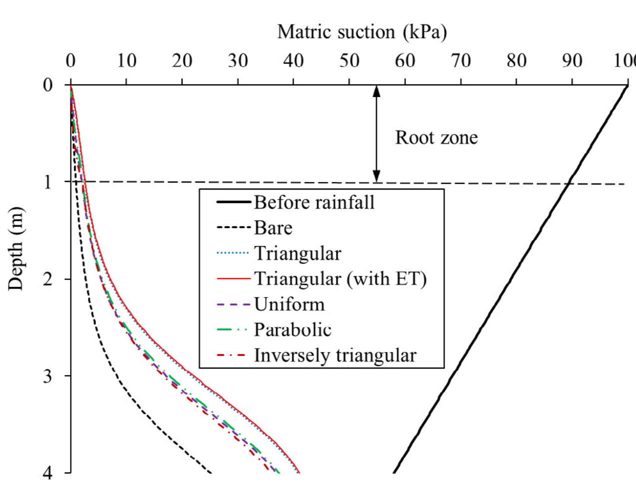

Fig. 7. Effects of R_v profiles on preserved suction after 24-h rainfall.

for both cases. These small differences are attributed to the small amount of actual transpiration (i.e., <0.5 mm) during the 2-h ponding event. The calculated total volume of root-water uptake within the root zone is less than 2.8×10^4 mm^3, which is negligible as it is 100 times smaller than the total volume of water infiltrated (i.e., >4.3×10^6 mm^3). Therefore, root-water uptake could not fully explain the observed suction preserved in the vegetated grounds. On the contrary, when root-induced changes in SWRC and $k(\psi)$ are both considered, the predicted suction profiles in both cases are closer to the measurements. This highlights the fact that during relatively short-duration wetting event, the root-induced changes in soil hydraulic properties is a crucial hydrological effect of vegetation that should not be neglected.

3.2. Effects of the shape of R_v on soil hydrology

Fig. 7 shows the computed suction profiles of the bare soil and the vegetated soils with the four different shapes of R_v after 24 h rainfall. Regardless of the shape of R_v, all four vegetated slopes preserve higher suction than the bare slope. Although most of the suction disappeared near the slope surface (up to a depth of 1 m), the suction preserved at deeper depth of 2 m in the vegetated slopes is 110% to 150% higher than that in the bare slope. The field studies presented by Simon and Collison [10] and Ni et al. [65] and the

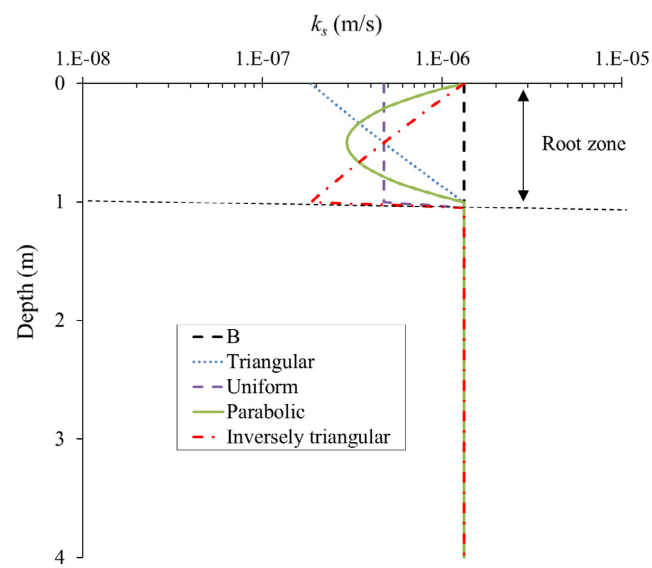

Fig. 8. Distribution of k_s along depth for different profiles of R_v.

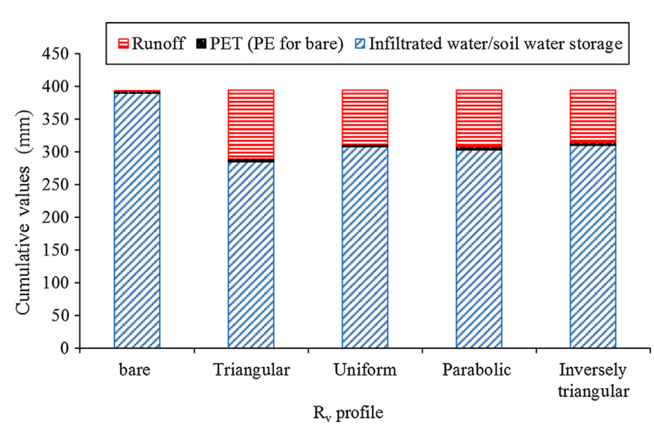

Fig. 9. Components of water balance in difference cases.

laboratory studies reported by Ng et al. [23] also found that the ability of vegetated soils to preserve matric suction is greater in deeper depths below the root zone.

Among the four different shapes of R_v, the triangular case shows a markedly greater ability for vegetated soil to preserve suction during rainfall, by 10–15 kPa when compared to the other three cases. No major difference of suction is found among the uniform, parabolic and inversely triangular cases. Interestingly, numerical simulations conducted by Ng et al. [66] conclude that during rainfall infiltration, the root architecture including the triangular case does not play a significant role in suction responses. It must be pointed that their simulation has assumed that the SWRC and $k(\psi)$ of bare and vegetated soils are identical to each other. The effects of root-induced changes in soil hydraulic properties had been ignored. Fig. 8 shows the distributions of k_s for different profiles of R_v. The four profiles of k_s have similar shape as the four profiles of R_v presented in Fig. 5. This is because, via Eqs. (3) and (6), k_s changes with e according to the shape of R_v. As shown in Fig. 8, the reduction of k_s in shallow root depth is the greatest for the triangular R_v profile. This hence leads to more surface runoff, resulting in a decrease in rainfall infiltration and consequently preserving higher suction in slopes during rainfall.

Another key observation from Fig. 7 is that when ET was considered during the prolonged 24 h rainfall, the suction profile has almost no difference from that without considering this. All components of water balance in each case are shown in Fig. 9. After raining for 24 h, the cumulative evaporation (for bare case) and ET (for all four vegetated cases) are less than 5 mm, which is negligible when compared to the amount of infiltration (in hundredths mm). The amount of water infiltration in all four vegetated cases is 20–27% lower than that in the bare case because of the root-induced reduction in k_s and partially due to the root-induced change in SWRC. In all calculations, the amount of water infiltrated is found to be the same as that stored in soil, as no bottom percolation took place throughout the rainfall event.

3.3. Effects of mechanical and hydrological reinforcements to slope stability

Fig. 10 shows the *FS* of the bare slope and the four vegetated slopes with different profiles of R_v, at the end of the 24 h rainfall event. It can be seen that the top 2.5 m of the bare slope is unsafe as the *FS* is less than 1.0. When only mechanical root reinforcement is taken into account, the *FS* in shallow depths increases significantly while that in deeper depths remain unchanged, as expected. Except the inversely triangular root distribution, only shallower soils up to 0.5 m depth could be stabilised when using the lower bound T_r. Soil at depths between 0.5 and about 2.5 m, where shallow landslip is usually of concerned, remains unstable for all cases. In Fig. 11, hydrological effects of plants (i.e., a combination of the effects of *ET* and root-induced changes in soil hydraulic properties) on *FS* are included. It can be seen that the hydrological effects also contributed partly to the slope stability in shallow depths, but in less extent as compared to deeper depths. The reason of having greater hydrological reinforcement effects (i.e., higher *FS*) in deeper depth is that the suction (hence shear strength) preserved after

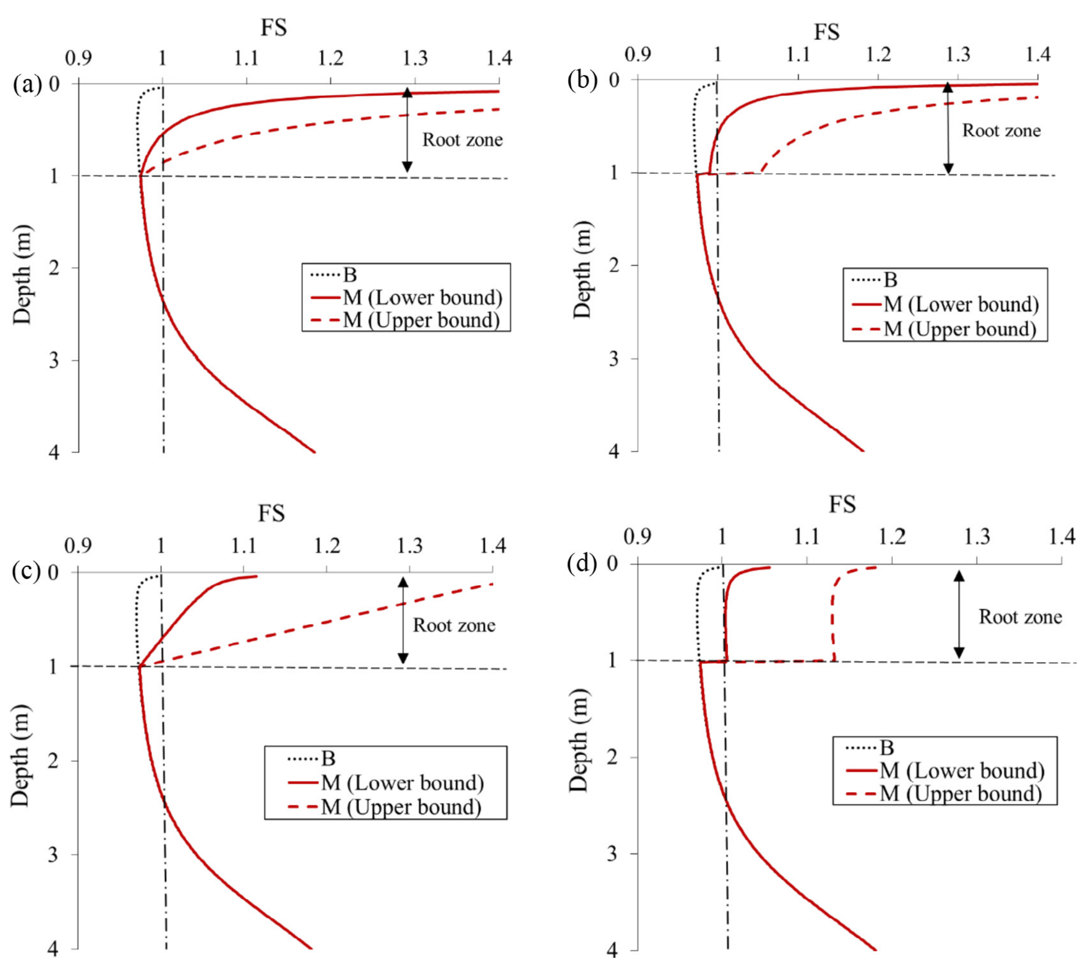

Fig. 10. Effects of mechanical reinforcement of vegetation on slope stability after 24-h rainfall for different R_v profiles; (a) Triangular; (b) Uniform; (c) Parabolic; and (d) Inversely triangular.

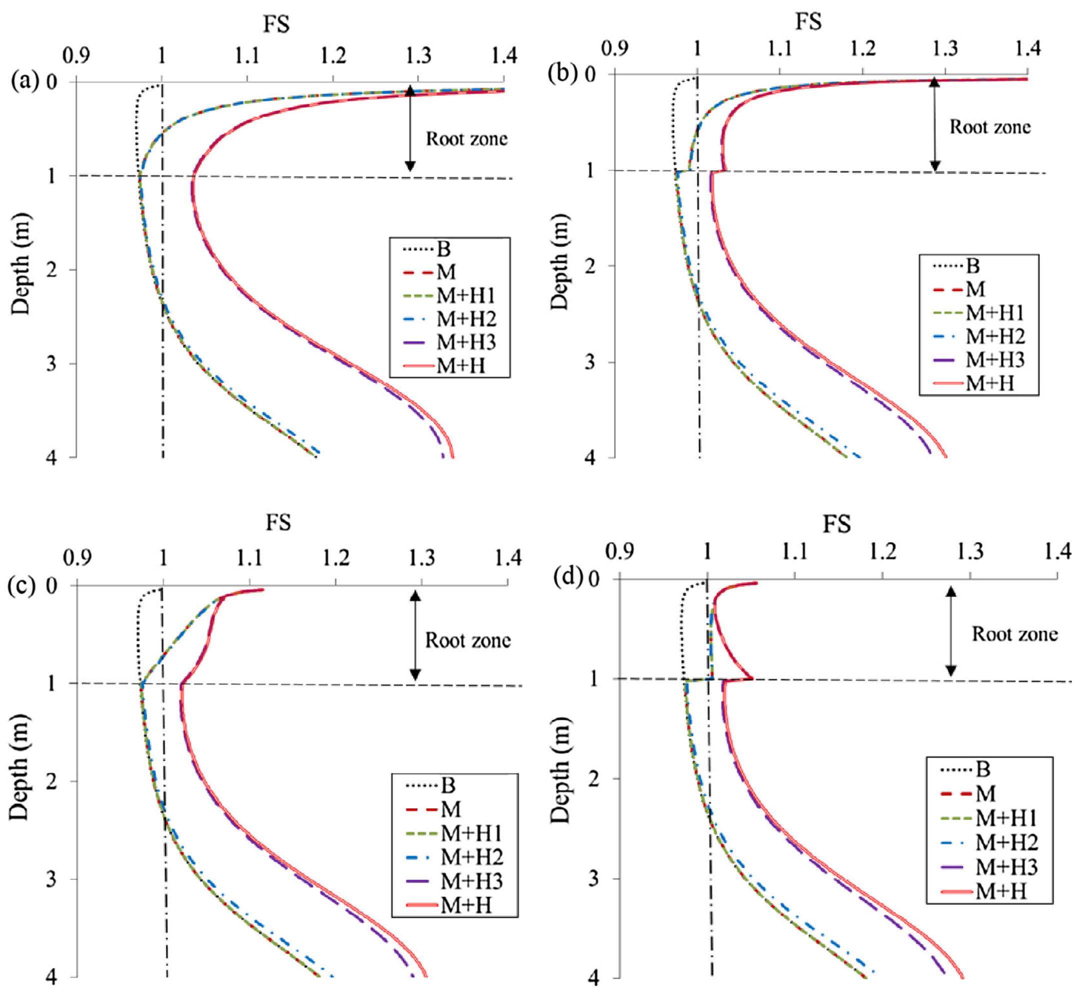

Fig. 11. Comparisons of the effects of hydrological and mechanical reinforcement (lower bound) of vegetation on slope stability after 24-h rainfall for different R_v profiles; (a) Triangular; (b) Uniform; (c) Parabolic; and (d) Inversely triangular. B is bare soil, M is mechanical root reinforcement; H1 is the effect of evapotranspiration; H2 is the effect of root-induced changes in SWRC, H3 is the effect of root-induced changes in k_s; and H considers all H1, H2 and H3.

rainfall is higher at depths below the root zone (see Fig. 7). This finding is consistent with various field measurements [65,67]. Fig. 11 also suggests that regardless of the shape of R_v, when all hydrological effects are ignored, only the top 0.5–1 m of the vegetated slope could be stabilised, depending on the shape of R_v. This has significantly underestimated the ability of vegetation for deeper slope stabilisation (up to 2.5 m) through the various mechanisms of hydrological reinforcements.

Since the *ET* during the 24 h rainfall event was minimal (see also Fig. 9), the removal of soil moisture through root-water uptake has only a negligibly small increase in the *FS*. In other words, *ET* effects on any slope stabilisation during rainfall might be practically ignored. On the other hand, although the presence of roots has shown to have some effects on SWRC (see Eqs. (3), (4) and Fig. 3), this particular hydrological mechanism appears not to contribute too much to slope stabilisation, though still greater than the effects of *ET*. Predominantly, the hydrological reinforcement is attributed to the root-induced change in k_s. Although this hydrological effect takes place only within the root zone (refer to Fig. 8), it has a significant effect on the soil hydrology for the entire soil profile.

When compared the four vegetated cases, no major difference of deep hydrological reinforcement is found. Consistently, the mechanism, root-induced changes in k_s, plays the most significant role in slope stabilisation in all four cases. Arguably, roots with a triangular R_v profile provide greater hydrological reinforcement below the root zone, but not very significantly compared to other R_v profiles. On the contrary, the shapes of R_v profiles have more significant impact on the shallow mechanical reinforcement. While both the triangular and uniform R_v profiles have strong stabilisation effects in very shallow depth (up to 0.5 m), the inversely triangular profile provides relatively less (i.e., less increase in *FS*) but has a much deeper influence depth (up to 1 m).

4. Discussion

The analyses have shown that the hydrological reinforcement is significant in depths that are relevant to slope stability problem (i.e., 1–2 m depth), rather than the shallow depth where matric suction would be largely dropped to zero after prolonged rainfall. It appears that root-induced changes in k_s plays the most prominent role compared to other hydrological effects. Previous studies [43,68,69] showed that the presence of roots does not necessarily cause a reduction of k_s. k_s of vegetated soil could be increased when roots die or decay due to aging [28,30] or competition of soil resources such as water due to close proximity of neighbouring plants [23,65]. These processes would create macro-pores, forming so-called root channels [70] for preferential water flow to take place and hence increasing hydraulic conductivity. To quantify the potential negative effects of root-induced increase in k_s, two

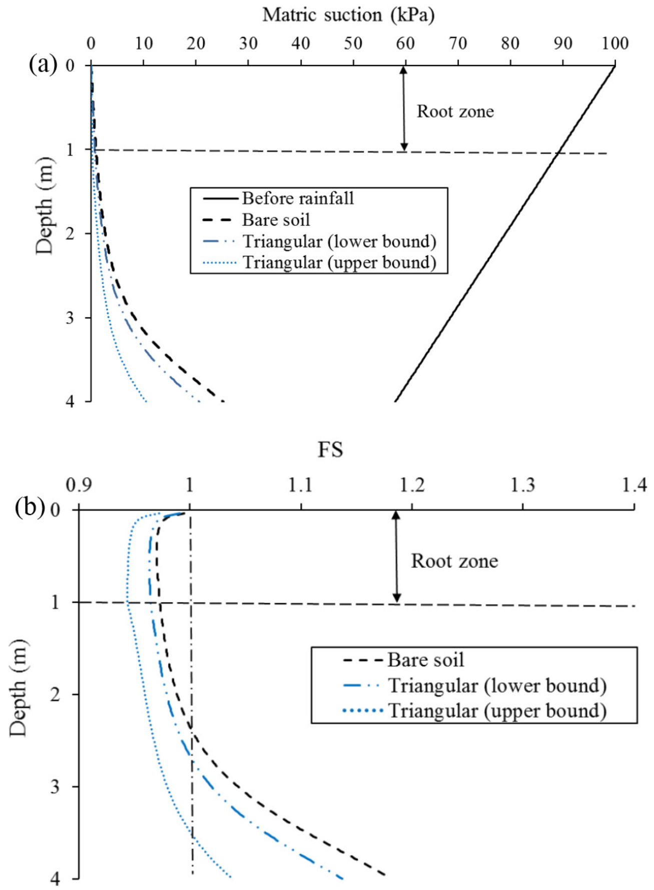

Fig. 12. Distribution of (a) matric suction preserved and (b) FS of the vegetated slope with a triangular profile of R_v after rainfall considering root-induced increase in k_s.

additional analyses were conducted by repeating the seepage and stability analyses of a vegetated slope which has a triangular R_v distribution. Based on the field and laboratory data, it is not uncommon to find a root-induced increase in k_s by 1.3–6.5 times due to root decaying/aging [23,28,30,71,72]. Thus, a lower and an upper bound calculation is conducted by setting the k_s within the root zone to be uniform and having a value of 1.3 k_s (Case VT2) and 6.5 k_s (Case VT3), respectively. Note that Case VT3 is an extreme condition where the plants were left to decay for 18 months [28].

Fig. 12(a) shows that suction preserved in these two cases was less than that in the bare slope for the entire 4 m depth. Consequently, the *FS* of the vegetated slope reduced (Fig. 12(b)). A larger amount of soil volume becomes unstable, as the slope depth where *FS* is less than 1.0 extends from 2.5 m (for bare case) to up to 3.5 m. It should be pointed out that the hydrological modelling made in this study considers vertical, 1D water flow. This represents the worst-case scenario as no lateral flow in the slope is permitted, "forcing" all infiltrated water to reduce pore-water pressure in deeper regions. The predicted suction preserved could thus be underestimated in these cases. Nevertheless, more research is needed to better quantify how much, and under what conditions, k_s of rooted soil would be increased or decreased, and hence how much the corresponding *FS* would be affected.

5. Conclusions

A numerical model is proposed and developed in this study to simultaneously consider the mechanical effects of root reinforcement and hydrological effects including (i) ET; (ii) root-induced change in soil water retention curve (SWRC) and (iii) root-induced change in saturated hydraulic conductivity (k_s), on the stability of an unsaturated vegetated coarse-grained soil slope. By comparing the model prediction with field data, considering only hydrological effect (i) is insufficient to predict matric suction in vegetated soils. Closer matches could be obtained when the other two hydrological effects (ii) and (iii) are taken into account.

Parametric study using the validated model shows that after a prolonged 24-h rainfall with a return period of 10 years, mechanical root reinforcement is effective to stabilise the shallow soil of up to 0.5 m depth generally, where most of the root biomass exists. On the contrary, hydrological reinforcement considering all the effects (i), (ii) and (iii) provides much significant effects of soil stabilisation in deeper depths (i.e., 1–2 m), where slip failure is normally of major concern. The presence of roots in a vegetated slope preserves higher suction, hence higher shear strength, after rainfall, as compared to a bare slope. It is identified that reduction in k_s due to the presence of intact roots (i.e., effect (iii)) is the most predominant hydrological effects. In contrast, increase in k_s due to the presence of dying/decaying roots could be detrimental to slope stability at 1–2 m depth due to the reduced ability of the vegetated slope to preserve suction. Other effects, in particular the root-water uptake through ET during rainfall, are minimal. Their contribution to slope stabilisation could be practically negligible.

The shape of the distribution of root volume ratio (R_v) within the root zone has a strong effect on shallow mechanical reinforcement, whereas no major difference is found in terms of deep hydrological reinforcement. Triangular and uniform R_v profiles provide strong mechanical stabilisation effects in shallow depth up to 0.5 m, while the inversely triangular profile gives a less stabilisation effect but has a much deeper influence depth of stabilisation, though generally less than 1 m.

Acknowledgements

We acknowledge research grants HKUST6/CRF/12R and T22-603/15N awarded by the Research Grants Council of the Government of the Hong Kong SAR. The second author acknowledges the EU Marie Curie Career Integration Grant under the project 'BioEPIC slope' and the research funding provided by the Engineering and Physical Sciences Research Council (EPSRC), UK (EP/N03287X/1).

References

[1] Wu TH, McKinnell WP, Swanston DN. Strength of tree roots and landslides on Prince of Wales Island, Alaska. Can Geotech J 1979;16(1):19–33.
[2] Pollen N, Simon A. Estimating the mechanical effects of riparian vegetation on stream bank stability using a fiber bundle model. Water Resour Res 2005;41:W07025.
[3] Fan CC, Su CF. Role of roots in the shear strength of root-reinforced soils with high moisture content. Ecol Eng 2008;33:157–66.
[4] Jotisankasa A, Taworn D. Direct shear testing of clayey sand reinforced with live stake. Geotech Test J, ASTM 2016;39(4):608–23.
[5] Greenwood JR, Norris JE, Wint J. Assessing the contribution of vegetation to slope stability. Proc Inst Civil Eng-Geotech Eng 2004;157(4):199–207.
[6] Genet M, Stokes A, Fourcaud T, Norris JE. The influence of plant diversity on slope stability in a moist evergreen deciduous forest. Ecol Eng 2010;36:265–75.
[7] Jotisankasa A, Mairaing W, Tansamrit S. Infiltration and stability of soil slope with vetiver grass subjected to rainfall from numerical modelling. In: Proceedings of the 6th International Conference on Unsaturated Soils: Research and Applications 2014, Sydney, Australia, 2–4 July 2014, pp. 1241–1247.
[8] Mao Z, Bourrier F, Stokes A, Fourcaud T. Three-dimensional modelling of slope stability in heterogeneous montane forest ecosystems. Ecol Eng 2014;273:11–22.
[9] Zhu H, Zhang LM, Xiao T, Li XY. Enhancement of slope stability by vegetation considering uncertainties in root distribution. Comput Geotech 2017;85:84–9.

[10] Simon A, Collison AJC. Quantifying the mechanical and hydrologic effects of riparian vegetation on streambank stability. Earth Surf Proc Land 2002;27(5):527–46.
[11] Leung FTY, Yan WM, Hau BCH, Tham LG. Root systems of native shrubs and trees in Hong Kong and their effects on enhancing slope stability. CATENA 2015;125:102–10.
[12] Pollen-Bankhead N, Simon A. Hydrologic and hydraulic effects of riparian root networks on streambank stability: is mechanical root-reinforcement the whole story. Geomorphology 2010;116(3–4):353–62.
[13] Leung AK, Ng CWW. Analysis of groundwater flow and plant evapotranspiration in a vegetated soil slope. Can Geotech J 2013;50(12):1204–18.
[14] Rahardjo H, Satyanaga A, Leong EC, Santoso VA, Ng YS. Performance of an instrumented slope covered with shrubs and deep-rooted grass. Soils Found 2014;54(3):417–25.
[15] Ng CWW, Kamchoom V, Leung AK. Centrifuge modelling of the effects of root geometry on transpiration-induced suction and stability of vegetated slopes. Landslide 2016. https://doi.org/10.1007/s10346-015-0645-7.
[16] Ng CWW, Leung AK, Yu R, Kamchoom V. Hydrological effects of live poles on transient seepage in an unsaturated soil slope: centrifuge and numerical study. J Geotech Geoenviron Eng 2016. 04016106-1.
[17] Tsiampousi A, Zdravkovic L, Potts DM. Numerical study of the effects of soil-atmosphere interaction on the stability and serviceability of cut slopes in London clay. Can Geotech J 2016;54(3):405–18.
[18] Soil Science Society of America. Glossary of Soil Science Terms. Madison, Wisconsin: Soil Science Society of America; 2008.
[19] Smethurst JA, Briggs KM, Powrie W, Ridley A, Butcher DJE. Mechanical and hydrological impacts of tree removal on a clay fill railway embankment. Géotechnique 2015;65(11):869–82.
[20] Leung AK, Garg A, Ng CWW. Effects of plant roots on soil-water retention and induced suction in vegetated soil. Eng Geol 2015;193:183–97.
[21] Garg A, Leung AK, Ng CWW. Comparisons of soil suction induced by evapotranspiration and transpiration of *S. heptaphylla*. Can Geotech J 2015;52(12):2149–55.
[22] Ng CWW, Woon KX, Leung AK, Chu LM. Experimental investigation of induced suction distribution in a grass-covered soil. Ecol Eng 2013;52:219–23.
[23] Ng CWW, Ni JJ, Leung AK, Zhou C, Wang ZJ. Effects of planting density on tree growth and induced soil suction. Géotechnique 2016;66(9):711–24.
[24] Ng CWW, Leung AK. Measurements of drying and wetting permeability functions using a new stress-controllable soil column. J Geotech Geoenviron Eng 2012;138(1):58–68.
[25] Ng CWW, Menzies B. Advanced unsaturated soil mechanics and engineering. London, UK: Taylor & Francis; 2007.
[26] Glendinning S, Loveridge F, Starr-Keddle RE, Bransby MF, Hughes PN. Role of vegetation in sustainability of infrastructure slopes. Proc Inst Civil Eng – Eng Sustain 2009;162(2):101–10.
[27] Ng CWW, Leung AK, Woon KX. Effect of soil density on grass-induced suction distributions in compacted soil subjected to rainfall. Can Geotech J 2014;51(3):311–21.
[28] Li Y, Ghodrati M. Preferential transport of nitrate through soil columns containing root channels. Soil Sci Soc Am J 1994;58:653–9.
[29] Scholl P, Leitner D, Kammerer G, Lioskandl W, Kaul HP, Bodner G. Root induced changes of effective 1D hydraulic properties in a soil column. Plant Soil 2014;381(1–2):193–213.
[30] Vergani C, Graf F. Soil permeability, aggregate stability and root growth: a pot experiment from a soil bioengineering perspective. Ecohydrology 2015. https://doi.org/10.1002/eco.1686.
[31] Ng CWW, Ni JJ, Leung AK, Wang ZJ. A new and simple water retention model for root-permeated soils. Géotechnique Lett 2016;6(1):106–11.
[32] Scanlan CA, Hinz C. Insight into the processes and effects of root induced changes to soil hydraulic properties. In: Proceedings of the 19th world congress of soil science, soil solutions for a changing world, Brisbane, Australia, 2010;2:41–44.
[33] Leung AK, Garg A, Coo JL, Ng CWW, Hau BCH. Effects of the roots of Cynodon dactylon and Shefflera heptaphylla on water infiltration rate and soil hydraulic conductivity. Hydrol Process 2015;29(15):3342–54.
[34] Liu HW, Feng S, Ng CWW. Analytical analysis of hydraulic effect of vegetation on shallow slope stability with different root architectures. Comput Geotech 2016;80:115–20.
[35] Feddes RA, Kowalik P, Kolinska-Malinka K, Zaradny H. Simulation of field water uptake by plants using a soil water dependent root extraction function. J Hydrol 1976;31(1):13–26.
[36] Feddes RA, Kowalik PJ, Zaradny H. Simulation of field water use and crop yield. Centre for Agricultural Publishing and Documentation; 1978.
[37] Jackson RB, Mooney HA, Schulze ED. A global budget for fine root biomass, surface area, and nutrient contents. Proc Natl Acad Sci 1997;94:7362–6.
[38] Gallipoli D, Wheeler SJ, Karstunen M. Modelling the variation of degree of saturation in a deformable unsaturated soil. Géotechnique 2003;3(1):105–12.
[39] van Genuchten MT. A closed-form equation for predicting the hydraulic conductivity of unsaturated soils. Soil Sci Soc Am J 1980;44(5):892–8.
[40] Veylon G, Ghestem M, Stokes A, Bernard A. Quantification of mechanical and hydric components of soil reinforcement by plant roots. Can Geotech J 2015;52(11):1839–49.
[41] Gish TJ, Jury WA. Effect of plant roots and root channels on solute transport. Trans Am Soc Agric Biol Eng 1983;26(2):440–4.
[42] Gabr MA, Akran M, Taylor HM. Effect of simulated roots on the permeability of silty soil. Geotech Test J 1995;18(1):112–5.
[43] Jotisankasa A, Sirirattanachat T. Effects of grass roots on soil-water retention curve and permeability function. Can Geotech J 2017. https://doi.org/10.1139/cgj-2016-0281.
[44] Yin JH. Influence of relative compaction on the hydraulic conductivity of completely decomposed granite in Hong Kong. Can Geotech J 2009;46(10):1229–35.
[45] Celia MA, Bouloutas ET, Zarba RL. A general mass-conservative numerical solution for the unsaturated flow equation. Water Resour Res 1990;26(7):1483–96.
[46] Vanapalli SK, Fredlund DG, Pufahl DE, Clifton AW. Model for the prediction of shear strength with respect to soil suction. Can Geotech J 1996;33(3):379–92.
[47] Hossain MA, Yin JH. Behaviour of a compacted decomposed granite soil from suction controlled direct shear tests. J Geotech Geoenviron Eng, ASCE 2010;136(1):189–98.
[48] Vanapalli SK. Shear strength of unsaturated soils and its applications in geotechnical engineering practice. In: Proc. of 4th Asia-Pacific Conference on Unsaturated Soils, New Castle, Australia, 2009; 579–598.
[49] Preti F. Schwarz M. On root reinforcement modelling. Geophysical Research 436 Abstracts, vol. 8, EGU General Assembly 2006, 2–7 April, ISSN: 1029–7006.
[50] Ritchie JT. Model for predicting evaporation from a row crop with incomplete cover. Water Resour Res 1972;8(5):1204–13.
[51] Garg A. Effects of vegetation types and characteristics on induced soil suction. PhD Thesis. The Hong Kong University of Science and Technology, Hong Kong; 2015.
[52] Watson DJ. Comparative physiological studies on the growth of field crops: I. Variation in net assimilation rate and leaf area between species and varieties and within and between years. Ann Botony 1947;11(1):41–76.
[53] Rasband WS. ImageJ. Bethesda, MD, USA: US National Institutes of Health; 2011.
[54] Rosenberg NJ. Microclimates: The Biological Environment. New York: Wiley; 1974.
[55] Allen RG, Pereira LS, Raes D, Smith M. Crop evapotranspiration. Guidelines for computing crop water requirements. Irrigation and Drainage Paper 56. FAO, Rome, Italy; 1998.
[56] Maass JM, Vose JM, Swank WT, Martinez-Zyrizar A. Seasonal changes of leaf area index (LAI) in a tropical deciduous forest in west Mexico. For Ecol Manage 1995;74:171–80.
[57] Nagler P, Glenn E, Nguyen U, Scott R, Doody T. Estimating riparian and agricultural actual evapotranspiration by reference evapotranspiration and modis enhanced vegetation index. Remote Sens 2013;5:3849–71.
[58] Penman HL. Natural evaporation from open water, bare soil and grass. Proc Roy Soc London 1948;193:120–46.
[59] GEO (Geotechnical Engineering Office). Technical guidelines on landscape treatment for slopes. Hong Kong, China: Geotechnical Engineering Office; 2011.
[60] Rahardjo H, Li XW, Toll DG, Leong EC. The effects of antecedent rainfall on slope stability. Geotech Geol Eng 2001;19:371–99.
[61] Hossain MA, Yin JH. Shear strength and dilative characteristics of an unsaturated compacted completely decomposed granite soil. Can Geotech J 2010;47(10):1112–26.
[62] Hau BCH, Corlett RT. Factors affecting the early survival and growth of native tree seedlings planted on a degraded hillside grassland in Hong Kong, China. Restor Ecol 2003;11(4):483–8.
[63] Leung AK, Kamchoom V, Ng CWW. Influences of root-induced soil suction and root geometry on slope stability: a centrifuge study. Can Geotech J 2017;54(3):291–303.
[64] Lam CC, Leung YK. Extreme rainfall statistics and design rainstorm profiles at selected locations in Hong Kong. Hong Kong: Royal Observatory; 1995.
[65] Ni JJ, Leung AK, Ng CWW. Investigation of plant growth and transpiration-induced suction under mixed grass-tree conditions. Can Geotech J 2017;54(4):561–73.
[66] Ng CWW, Liu HW, Feng S. Analytical solutions for calculating pore water pressure in an infinite unsaturated slope with different root architectures. Can Geotech J 2015;52:1–12.
[67] Garg A, Coo JL, Ng CWW. Field study on influence of root characteristics on suction distributions in slopes vegetated with *Cynodon dactylon* and *Schefflera heptaphylla*. Earth Surf Proc Land 2015;40(12):1631–43.
[68] Murphy B, Koen T, Jones B, Huxedurp L. Temporal variation of hydraulic properties for some soils with fragile structure. Aust J Soil Res 1993;31(2):179–97.
[69] Kristopher DB, Daryl FD. Two-year performance by evapotranspiration covers for municipal solid waste landfills in northwest Ohio. Waste Manage 2012;32:2336–41.
[70] Ghestem M, Sidle RC, Stokes A. The influence of plant root systems on subsurface flow: implications for slope stability. Bioscience 2012;61(11):869–79.
[71] Rasse DP, Smucker AJM, Santos D. Alfalfa root and shoot mulching effects on soil hydraulic properties and aggregation. Soil Sci Soc Am J 2000;64(2):725–31.
[72] Scanlan CA. Processes and effects of root-induced changes to soil hydraulic properties. PhD Thesis. University of Western Australia; 2009.